

Microfluidic Biomaterials

Joe Tien* and Yoseph W. Dance

Since their initial description in 2005, biomaterials that are patterned to contain microfluidic networks (“microfluidic biomaterials”) have emerged as promising scaffolds for a variety of tissue engineering and related applications. This class of materials is characterized by the ability to be readily perfused. Transport and exchange of solutes within microfluidic biomaterials is governed by convection within channels and diffusion between channels and the biomaterial bulk. Numerous strategies have been developed for creating microfluidic biomaterials, including micromolding, photopatterning, and 3D printing. In turn, these materials have been used in many applications that benefit from the ability to perfuse a scaffold, including the engineering of blood and lymphatic microvessels, epithelial tubes, and cell-laden tissues. This article reviews the current state of the field and suggests new areas of exploration for this unique class of materials.

microfluidic device for potential biological applications.^[7] These so-called “microfluidic biomaterials” were originally developed in alginate hydrogels by Abe Stroock’s group in 2005^[8] and have since seen a tremendous increase in attention as the advantages of these materials for tissue engineering and drug delivery have become better appreciated.

1.1. Core Features of Microfluidic Biomaterials

A microfluidic biomaterial is a biomaterial (most commonly, a hydrogel such as alginate or type I collagen) that contains a microscale channel that can sustain fluid flow. The material should be compatible

with the culture of cells *within* the bulk of the material. As in more traditional microfluidic devices, the channel widths in microfluidic biomaterials are expected to be below 1 mm. Thus, microfluidic biomaterials are porous at two or more length scales: one that characterizes the channel widths, and a smaller one that characterizes the average pore size of the biomaterial bulk. Depending on how the biomaterial bulk is synthesized, the latter scale can be orders-of-magnitude smaller than that of the channels.

Microfluidic biomaterials possess many advantages for potential biological applications. First, and most importantly, these materials are inherently able to sustain fluid flow. As a result, immediate perfusion is possible, which is desirable when the biomaterial contains embedded cells to which nutrients are to be delivered and from which metabolites are to be removed. In the absence of perfusion, solute transport can only occur via diffusion, which becomes prohibitively slow for millimeter-scale materials. Second, the transport of substances and/or cells to and from the biomaterial can be tailored with the geometry of the microfluidic network.^[9] For a given external driving pressure, the local channel density and flow rate dictate the rate at which solutes can be exchanged between the perfusing fluid and the material bulk. Third, because the sizes and locations of microfluidic channels are chosen by design, the microfluidic geometry within the biomaterial is well-controlled and reproducible. This characteristic makes the flow distribution within the network predictable and the solute transport amenable to computational modeling. Fourth, microfluidic biomaterials contain micrometer-scale channel widths that are particularly well-suited for replicating the geometry of microvessels and other tubular structures that are desired in engineered tissues.^[10,11]

In nearly all implementations to date, the microfluidic geometry is *open*. That is, the channel(s) span the entire extent of the biomaterial, so that fluid can enter and exit the channel via

1. Introduction

The development of microfluidic technology has revolutionized biochemical assays by increasing their speed and sensitivity and by decreasing the volumes of reagents that they require.^[1,2] The small length scales and large surface area-to-volume ratios that are inherent to microfluidic devices reduce typical solute transport times and increase the rate of binding events.^[3,4] Although originally envisioned for miniaturization of standard large-scale laboratory assays, the field of microfluidics has expanded to include devices that take advantage of physicochemical phenomena that emerge only at small length scales.^[5]

Commercial microfluidic devices are primarily etched and/or molded from mechanically sturdy and chemically durable materials, such as glass, polydimethylsiloxane (PDMS), and thermoplastics.^[1,2] The spectacular success of glass- and polymer-based microfluidics in biochemical analyses and related applications has led to the investigation of microfluidic systems in other classes of materials.^[6] These efforts have led to the invention of a new type of biomaterial that doubles as a

Prof. J. Tien, Y. W. Dance
Department of Biomedical Engineering
Boston University
Boston, MA 02215, USA
E-mail: jtien@bu.edu

Prof. J. Tien
Division of Materials Science and Engineering
Boston University
Boston MA 02215, USA

 The ORCID identification number(s) for the author(s) of this article can be found under <https://doi.org/10.1002/adhm.202001028>

DOI: 10.1002/adhm.202001028

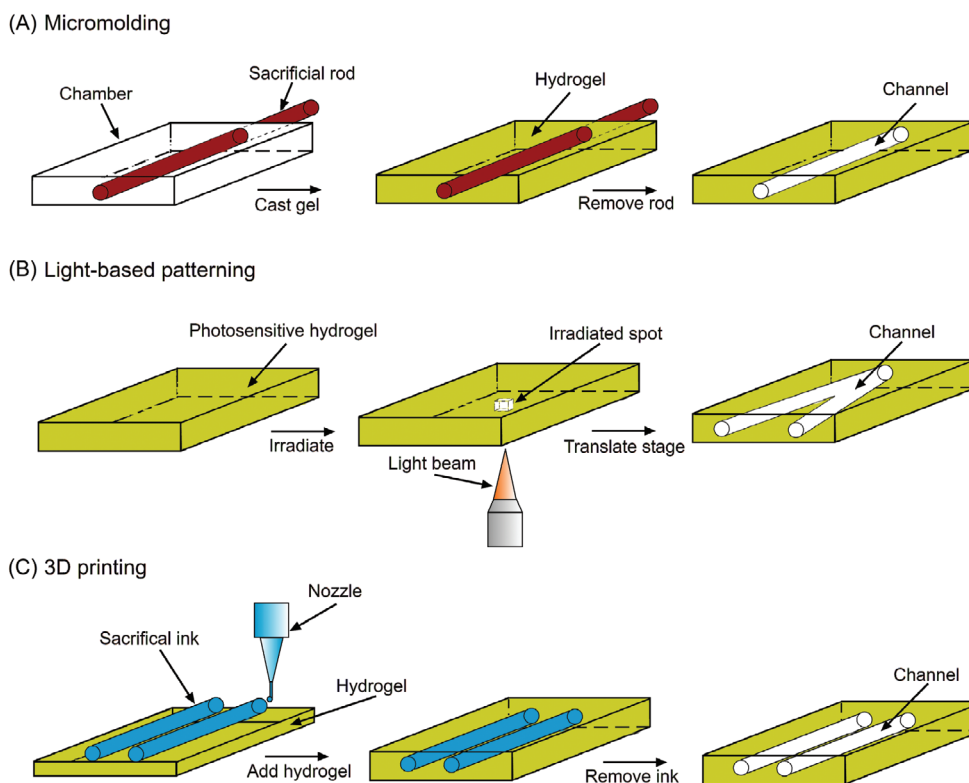


Figure 1. Strategies for forming microfluidic biomaterials and representative implementations. A) Micromolding: Generation of a channel by removal of a thin rod from bulk material. B) Photopatterning: Generation of channels by patterned laser ablation of bulk material. C) 3D printing: Generation of channels by dissolution of a 3D-printed structure within a bulk material.

viscous laminar flow.^[9,12–15] Flow through the material proceeds in parallel across spanning channels and through interconnected pores within the bulk. Because the resistance to flow is much smaller in the channels compared to that through the material pores, the vast fraction of flow is driven preferentially through the channels. This type of fluidic operation mimics that of biological distribution networks, such as the blood microvascular system, and is designed for efficient delivery and removal of solutes to and from the material bulk.

A less common implementation is to make the microfluidic geometry *semi-open*. Here, the channel(s) are open at one end, but remain closed (i.e., blind-ended) at the other end.^[16,17] As a result, fluid can enter or exit a channel at the open end, but it must disperse from the channel into the pores of the biomaterial bulk at the blind end. Because all flow in semi-open networks must proceed at some point through the pores, the flow resistance is much higher than for the case of open microfluidic geometries. The blind-ended geometry is intended to mimic the tree-like networks that are found in many biological tissues, such as the lymphatic system and branching epithelial networks.

1.2. Scope of the Review

This review describes strategies to engineer microfluidic biomaterials and examples of how this class of biomaterials has been applied in tissue engineering (particularly for “microflu-

idic vascularization”) and in drug delivery. Given the focus of this special journal issue, the contributions of former Whitesides Group members to this field are noted. This review is limited to studies in which the channel geometries are engineered by design. Thus, the creation of microfluidic scaffolds from natural tissues, such as whole animal organs^[18,19] or the leaves of a plant,^[20] will not be discussed. The much larger field of microphysiological systems lies well outside the scope of this paper, and the interested reader is referred to outstanding recent reviews.^[21,22]

2. Methods for Forming Microfluidic Biomaterials

Methods for engineering microfluidic biomaterials can be grouped into categories that reflect both the patterning method itself and the types of microfluidic geometries that are achievable (Figure 1). The first, and most commonly applied, strategy is based on micromolding of hydrogels (Figure 1A). This approach is amenable to the formation of gels that contain single channels or planar networks. It is widely used by many research groups, in large part because the underlying techniques can be implemented without access to specialized equipment. A second strategy is based on using light to pattern the material of interest (Figure 1B). Light-based approaches are more geometrically versatile than those based on micromolding and are able to form quasi-planar networks. Finally, and most recently, 3D printing

has emerged as perhaps the best candidate for generating true 3D networks (Figure 1C). Both light- and printing-based methods require specialized motors and stages to move the light source or printing nozzle precisely relative to the existing pattern in a biomaterial.

Aside from micromolding, photopatterning, and 3D printing, other less common methods for forming microfluidic biomaterials have been developed. These methods are capable of generating an open microfluidic structure, but are often limited in the types of microfluidic geometries and spatial resolutions that can be achieved. Of these methods, the one based on viscous fingering^[23] is perhaps the best known, and it will be discussed at the end of this section.

2.1. Micromolding

Microfluidic biomaterials can be formed by micromolding of the material against a pre-patterned template. This strategy is a direct extension of the use of silicone (PDMS) stamps for micromolding of thermosetting or UV-curable polymers.^[24] This approach is suitable for biomaterials that can be converted from a liquid form into a rigidified mass. Hydrogels, both natural and synthetic, are the most common type of biomaterial used with micromolding. Hydrogels have the particular advantage that they are inherently porous and can serve as mimics of the extracellular matrix, so the resulting microfluidic gel is well-suited as a scaffold for engineering living tissues. The first example of a microfluidic biomaterial, reported in 2005, was formed by micromolding of alginate gels.^[8]

Micromolding-based methods are arguably the most popular ones for generating microfluidic biomaterials. This popularity stems in part because these methods are analogous to those normally used in PDMS-based soft lithography. They are technically not too demanding and are easy to learn. Although in principle micromolding can be automated, it is largely implemented as a technique for manual production of small numbers of samples. It is ideal for creating scaffolds for microphysiological systems with relatively simple network geometries.

2.1.1. Subtractive Approaches

“Subtractive” approaches to molding microfluidic biomaterials refer to methods in which the removal of a pre-patterned element results in the creation of the microfluidic channel or network.^[25] In the most common implementation of the subtractive approach, a thin solid cylindrical rod serves as the sacrificial element.^[12] The rods can be made of stainless steel,^[12] for which perfectly straight acupuncture needles are available, down to 100 μm in diameter. The steel needles can be etched chemically to 20–30 μm in diameter. The rods can also be made from glass that is formed in a pipette puller, down to ≈ 5 μm in diameter.^[26] The finer the rod, the more likely it is to bend under lateral forces, and one must be careful if the goal is to obtain channels in the same plane. Flexible PDMS rods, appropriately supported, have also been used as the removable element.^[27]

Open perfusable channels are obtained when the hydrogel is added selectively around the mid-section of the rod before removal of the rod. To decrease adhesion between the rod and subsequently added hydrogel, pre-adsorption of serum albumin onto

the rod is helpful.^[28] The rod is typically held by a rigid guide that ensures the smooth and true removal of the element. Especially for thinner channels, any vibration in the rod as it is removed will lead to poor resolution of the channel. Detailed protocols have been published to assist in troubleshooting this type of patterning.^[25] Blind-ended cavities are obtained when sufficient hydrogel is added to cover the tip of the rod before removal of the rod.

Two or more rods can be used together to generate more complex microfluidic geometries or operating conditions. For instance, a parallel array of rods can be used to generate a parallel array of channels.^[29,30] Similarly, an arrangement of two rods in the form of a “T” (one rod forming the top of the “T,” the other forming the centerline) can be used to create separate perfused and blind-ended channels within a single biomaterial.^[29] In principle, each channel can be separately perfused, which enables generation of pressure and chemical gradients within the biomaterial.^[30]

Because it is based on manual extraction of the patterning element, the rod-based subtractive approach can be applied to essentially any hydrogel, such as type I collagen, fibrin, gelatin, silk fibroin, and polyethylene glycol.^[12,31–33] The versatility of this approach has led to the availability of at least one commercial product (the ParVivo microfluidic chip by Nortis) that provides a pre-assembled, ready-to-use setup, *sans* hydrogel, with an ≈ 120 μm diameter silica microfiber as the subtractive element for each device.

The rod-based approach is chiefly used to generate individual single channels, although clever implementations have obtained branching networks from manual removal of flexible PDMS or agarose elements.^[27,33] To create interconnected networks, the standard approach is to use micromolded meshes as the sacrificial element. Once the mesh is partially encapsulated by the hydrogel, the mesh can be removed (e.g., by melting or dissolving) to leave behind a microfluidic network (Figure 2A). The sacrificial meshes with the finest resolution (≈ 5 μm) appear to be those made from gelatin, as we reported in 2007.^[34] Gelatin can be molded at high concentrations that result in mechanically sturdy meshes; since the gelation is thermoreversible, the gelatin mesh can be readily removed by melting and flushing. Stacking of sacrificial gelatin has been used to generate sacrificial elements that can yield independent serpentine channels.^[35] Alginate can also be molded into a sacrificial mesh, which can be removed by immersion in a calcium ion chelator.^[36] Because the meshes are typically molded against PDMS stamps that are cast against sharp photoresist patterns, the resulting microfluidic networks have rectangular cross-sections.

Whether made by molding around rods or a patterned mesh, the resulting biomaterial is monolithic (i.e., there are no welds or adhesion planes) and thus structurally as robust as a bulk version of the material. This property is particularly advantageous when perfusing the channels at high pressure; previous work has shown fracture strengths in excess of 60–200 mm Hg.^[34,36] A second advantage of the subtractive approach is that it is widely applicable to many different types of biomaterials. As long as the method of removing the sacrificial element does not interfere with the surrounding bulk biomaterial, this approach is virtually guaranteed to yield the desired structure.

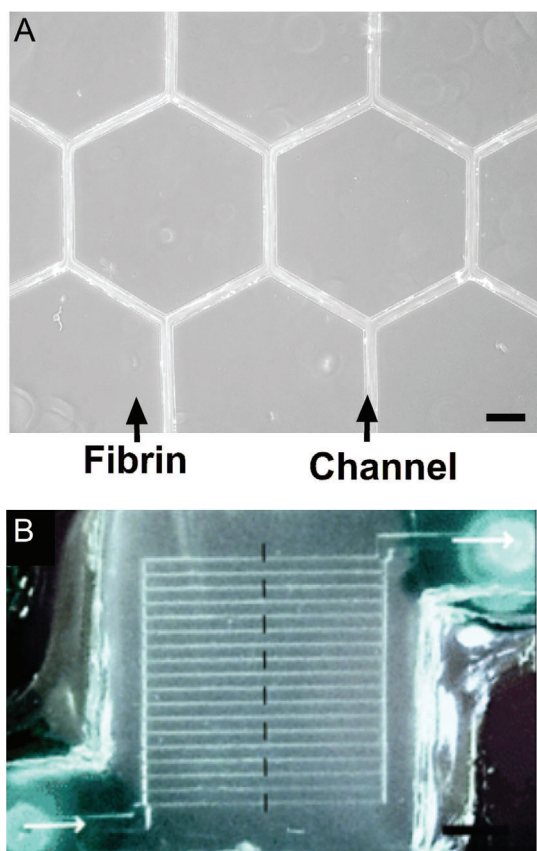


Figure 2. Formation of microfluidic biomaterials by micromolding. A) Subtractive approach: Fibrin gel with an internal hexagonal network that remained after removal of a gelatin mesh. The gel is perfused with 1 μm diameter microspheres. Scale bar refers to 200 μm . Adapted with permission.^[34] Copyright 2007, Royal Society of Chemistry. B) Additive approach: Alginate gel that was bonded with transient exposure to citrate to contain a grid-like network. Scale bar refers to 2.5 mm. Adapted with permission.^[8] Copyright 2005, American Chemical Society.

2.1.2. Additive Approaches

“Additive” approaches to molding microfluidic biomaterials refer to methods in which two or more molded biomaterials are bonded to form the microfluidic structure. The challenge of ensuring that bonding is sufficiently strong to resist internal pressurization of the channels is inherent to the additive strategy.

In the most straightforward implementation of the additive approach, the microfluidic material is formed by bonding one flat (i.e., unpatterned) gel with a molded one that contains an indentation in the shape of the network.^[8,37,38] Again, the use of gels that are molded against PDMS stamps results in microfluidic geometries that have sharp corners. To obtain cylindrical channels through an additive approach, in principle it is possible to bond two gels that have hemi-cylindrical indentations. This approach is technically more demanding, as it requires careful alignment of the gels before bonding.

For ionically crosslinked biomaterials, such as alginate, bonding can be induced by transiently removing the relevant ion. This strategy was the one taken by Stroock’s group in their re-

port of the first microfluidic biomaterial (Figure 2B).^[8] When two molded alginate gels are placed into contact and then transiently exposed to citrate (to chelate calcium ion), the initial weak bond based on passive adhesion is transformed into a strong bond based on re-assembly and interpenetration of alginate fibers at the interface.

For fibrous self-assembling biomaterials, such as collagen or fibrin gels, bonding can be induced by transient exposure to high concentrations of low-molecular-weight “perturbants,” such as urea or guanidinium ion.^[37] These molecules disrupt the structure of the hydrogel (at sufficiently high concentrations, they completely liquefy a preformed gel). Without the intermediate bonding step, two patterned collagen or fibrin gels that are initially adherent can detach under repeated mechanical deformation, such as manipulation with tweezers or contraction by adherent cells. Other types of gels can be bonded thermally.^[39,40]

In contrast to the materials versatility of the subtractive approach, the additive approach requires each material to be treated with its own tailored bonding recipe (e.g., citrate for alginate, perturbants for collagen). In all of these bonding strategies, a balance must be struck between adhesion and spatial resolution: stronger bonding regimens (i.e., greater concentration of bonding agent, longer treatment time) will result in greater adhesion between gels, but at the cost of blurring the sharp features on the pre-patterned gels.

Bond strengths can be made sufficiently high that the resulting microfluidic networks are mechanically stable. Although it is unclear whether the mechanical strength of additively bonded microfluidic biomaterials can equal that of subtractively generated ones, the strength appears to be sufficient for most practical applications *in vitro* and possibly *in vivo*. For gels that are sufficiently stiff, a bonding step may not be needed to yield a microfluidic structure that remains intact under environmental stresses.^[41]

In principle, the additive approach can be used to build biomaterials with an internal 3D microfluidic network layer-by-layer, as has been demonstrated with PDMS-based microfluidics.^[42] So far, however, routine extension of the layer-by-layer approach from PDMS to hydrogels remains elusive. Alignment of deformable gels has proven to be far more challenging than that of comparatively rigid PDMS.

2.2. Light-Based Methods

The absorption of light can also be used to generate microfluidic biomaterials in a subtractive or additive process. Because the materials of interest (e.g., hydrogels) are typically transparent, using light as the patterning agent means that the patterning step is no longer limited to the outer surface of a material, as it would be for micromolding. The major advantage of light-based techniques is their ability to create arbitrary, complex microfluidic geometries, such as branched structures or 3D networks. Because these methods are often implemented through a microscope, the networks tend to be quasi-planar. The speed of the patterning technique is governed by the dwell time of the light beam per voxel within the to-be-patterned material. As a result, light-based methods require a trade-off between patterning resolution and speed. Simultaneous exposure through multiple light beams

(e.g., with a digital mirror array^[43]) can potentially improve patterning speed without loss of resolution.

2.2.1. Microfluidic Biomaterials via Photodegradation

Photodegradation is a subtractive approach to creating microfluidic biomaterials, in which light is used to remove material where the channels are to be formed. Thus, the material acts like a positive photoresist. In most cases, photodegradation requires a bulk transparent hydrogel to be irradiated at a wavelength that is tailored to the specific photosensitive moiety in the backbone of the hydrogel. Thus, this approach is particularly well-suited to synthetic gels, such as those made from polyethylene glycol (PEG) and its derivatives, in which the desired photolabile group can be readily introduced.^[44,45]

One of the main limitations with using photosensitive PEG gels is that PEG by itself lacks the adhesive moieties that allow cells to grow well within the bulk gel or on the surface of a channel. Given that much of the driving force for the development of microfluidic biomaterials has been the desire to create new scaffolds for engineered tissues, the biological inertness of PEG poses a major problem. This issue can be overcome by coupling adhesive peptides (such as GRGDS) to the gel after photodegradation.

In practice, the photodegradation takes place by focusing the light through a microscope objective onto the biomaterial and translating the focal point in the desired pattern. Single-photon widefield microscopes cause significant excitation outside of the focal plane, which can lower the resolution of the resulting pattern. Multiphoton microscopes minimize out-of-plane excitation and thus increase the patterning resolution, but at the cost of a larger excitation intensity. Much of the advances in this approach require the combination of improvements in material photochemistry (e.g., higher absorption cross-sections) and microscope capability.

Light can also be used to create microfluidic networks within nonphotolabile hydrogels, such as type I collagen (**Figure 3A**). Here, the light is not tuned to a specific wavelength for the degradation of a particular chemical moiety. Rather, high-intensity pulsed laser illumination is used to cleave essentially all the covalent bonds in the exposed region. Because this method uses non-specific photoablation, it can be applied to a wide variety of materials, including protein and polymer gels.^[15,46–48] On the other hand, it requires higher energies than degradation of photosensitive materials does; with care, these energies do not appear to be harmful to cells outside the illuminated region.^[47] In one study, light was used to deliberately ablate both collagen and cells, which led to enhanced cell migration into the resulting channels.^[48]

2.2.2. Microfluidic Biomaterials via Photopolymerization

In photopolymerization, the biomaterial serves as a negative photoresist and is built up layer-by-layer to create the channel(s). This approach is similar to resin-based stereolithography, which generates 3D structures by scanning a laser across the surface of a photosensitive liquid resin as the liquid is translated vertically. As with photodegradation, PEG-based gels can be used in photopolymerization to form microfluidic channels.^[50,51] Designed with

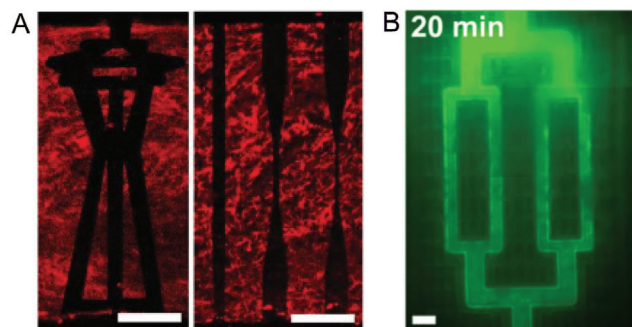


Figure 3. Formation of microfluidic biomaterials with light-based patterning. A) Photodegradation: Collagen gel that contains open segments formed by photoablation, viewed with second harmonic generation. Dark areas represent collagen-free regions. Scale bar refers to 100 μm . Reproduced with permission.^[48] Copyright 2020, AAAS. B) Photopolymerization: Citric-acid based biodegradable elastomer that contains a microfluidic network, after perfusion with a solution of fluorescein. Scale bar refers to 300 μm . Reproduced with permission.^[49] Copyright 2016, Springer Nature.

the appropriate wavelength sensitivity, the photosensitive groups are intended to form crosslinks between PEG chains. Photopolymerization has also been used with biodegradable elastomers to form microfluidic channels (**Figure 3B**).^[49]

Although it may seem as if photodegradation and photopolymerization are just two sides of the same coin, they differ practically in several ways. Photodegradation is applied to an initially crosslinked, rigid gel; breaking bonds is localized exclusively to regions that have absorbed sufficient light. In contrast, photopolymerization is applied to a liquid precursor that is then selectively crosslinked. Since the photosensitive precursor is not rigid during the illumination, the resolution of photopolymerization can suffer if the crosslinking agent can diffuse (e.g., from polymer reptation) or in the presence of mechanical vibration. With photodegradation, the most strongly illuminated region is fully degraded, and surrounding regions are partially degraded from scattered or unfocused light. With photopolymerization, it is tricky to ensure that the region that is intended to be a channel remains fully unpolymerized. To improve the feature resolution that is achievable with photopolymerization, in practice each layer is often formed separately before being assembled into the microfluidic structure.

2.3. 3D Printing

In 3D printing, either a sacrificial material or the biomaterial itself is extruded from specially designed nozzles into the desired pattern. This strategy is currently one of the most promising for generation of large, organ-scale microfluidic biomaterials. Similar to the rod-based micromolding methods, 3D printing is a physical patterning technique. As a result, it is extremely versatile in terms of the materials used. Unlike photopatterning, it does not require the development of specialized chemistries. The power of 3D printing is in its spatial versatility, as the print nozzles can be moved “freeform” in 3D with virtually no limitations. Although the current resolution of 3D printers does not match what can be achieved with micromolding or with light, much

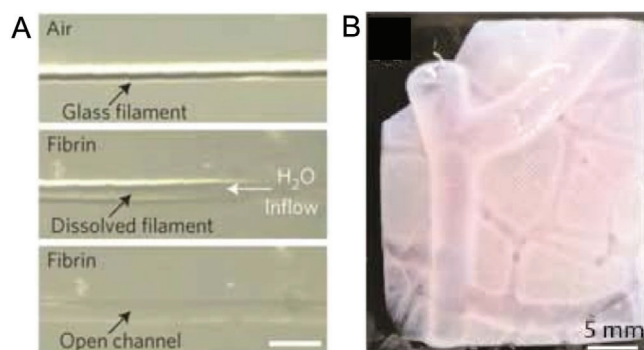


Figure 4. Formation of microfluidic biomaterials with 3D printing. A) Sacrificial approach: Fibrin gel that contains a channel formed by dissolution of a printed sugar filament. Scale bar refers to 500 μm . Reproduced with permission.^[173] Copyright 2012, Springer Nature. B) Additive approach: Collagen gel that contains a biomimetic microfluidic network directly printed into a gelatin-based support bath. Adapted with permission.^[53] Copyright 2019, AAAS.

attention in biomaterials research is now focused on this technology, and further improvements are very likely.

2.3.1. Direct Writing of Sacrificial Materials

3D printing can be used to manually write sacrificial materials with micrometer-scale resolution. These materials can be partially encapsulated in a biomaterial, and then removed to yield a microfluidic network in the biomaterial (Figure 4A). This method is the 3D analog of the use of micromolded sacrificial meshes described earlier, and it displays the same materials versatility of subtractive micromolding techniques.

Several types of sacrificial “inks” have been studied, with variations in the types of structures that are achievable. As Chris Chen’s group showed in 2012, inks that consist of concentrated sugar-based solutions can be used to print freestanding 3D sacrificial meshes.^[13] This printing process takes advantage of the ability of a sugar solution to dry into a rigid glassy filament upon extrusion from the print nozzle into air. These filaments can be printed into open 3D meshes that are sturdy enough to be shipped intact between laboratories. Because sugar mesh dissolves readily in water, using it as the sacrificial element for microfluidic hydrogels requires that the filaments be pre-coated with a thin layer of degradable (i.e., hydrolytically metastable) polymer to temporarily stabilize the filaments against dissolution.

A second major class of inks are based on thermoreversible Pluronic block copolymers of PEG and polypropylene glycol.^[52] These polymers display temperature-dependent behavior that is essential to their use as inks. In particular, Pluronic undergoes a sol-to-gel phase transition when heated above a critical temperature that depends on the molecular weights of the two polymer blocks. Concentrated Pluronic solutions can be printed into warm aqueous baths, encapsulated in the biomaterial of interest, and then liquefied and flushed out in the cold.^[52,54] Other types of thermoreversible inks, such as concentrated gelatin, can be 3D-printed and used to create microfluidic materials in a similar manner.^[55,56] It is even possible to print an ink of lightly

crosslinked gelatin methacrylate, which degrades quickly to yield a channel in a surrounding matrix.^[57]

The resolution of subtractive approaches based on 3D-printed sacrificial elements depends on the speed of extrusion from the printer nozzle, the diameter of the nozzle opening, and the viscoelastic properties of the ink. Higher extrusion speeds yield thinner and flimsier filaments. Structures as fine as ≈ 150 and ≈ 45 μm in diameter have been reported with sugar-based glass and Pluronic copolymers, respectively.^[13,52]

2.3.2. Additive 3D Printing

It is possible to print a microfluidic biomaterial additively from a precursor gel, with or without embedded cells (Figure 4B). Early implementations suffered from poor resolution, as the printed gel precursor can spread onto existing layers before gelation occurs. Recent studies have shown that printing into a Bingham plastic fluid allows the fluid to support the printed structures.^[53,58] With an optimized support bath, direct 3D printing can be used to create channels down to ≈ 100 μm in diameter.^[53] Extension of this approach to even smaller channels appears possible with the development of fine-grained support baths.

2.4. Nonlithographic Approaches

Although micromolding, photodegradation/polymerization, and 3D printing are the most commonly investigated techniques for generating microfluidic biomaterials, other approaches have been tried, with some success. These approaches tend to be more restricted in the types of materials and/or microfluidic geometries that they are suitable for. In exchange, they provide ease of use that enables a quick and convenient generation of microfluidic channels.

2.4.1. Viscous Fingering

Of the alternatives, viscous fingering is the one that has seen the most application.^[23,59] This technique takes advantage of the Taylor instability that occurs when a less viscous fluid is pressurized against a more viscous one.^[60] The instability at the interface between the two fluids can result in focusing of the less viscous one into a thin stream that displaces the more viscous fluid only in the stream. Application of this phenomenon toward forming a microfluidic biomaterial starts with filling a microfluidic chamber with a viscous, liquid precursor to the biomaterial. When less viscous saline is added upstream of the precursor under hydrostatic pressure, the precursor is displaced only along a thin, central stream. The precursor can then be gelled with the channel intact.

The advantage of this approach is its unmatched simplicity. Viscous fingering is even simpler to implement than micromolding, and certainly when compared to photopatterning or 3D printing. The patterning step can be driven by gravity or surface tension.^[23,59] Moreover, viscous fingering can generate single channels or branched junctions, and the resulting biomaterial

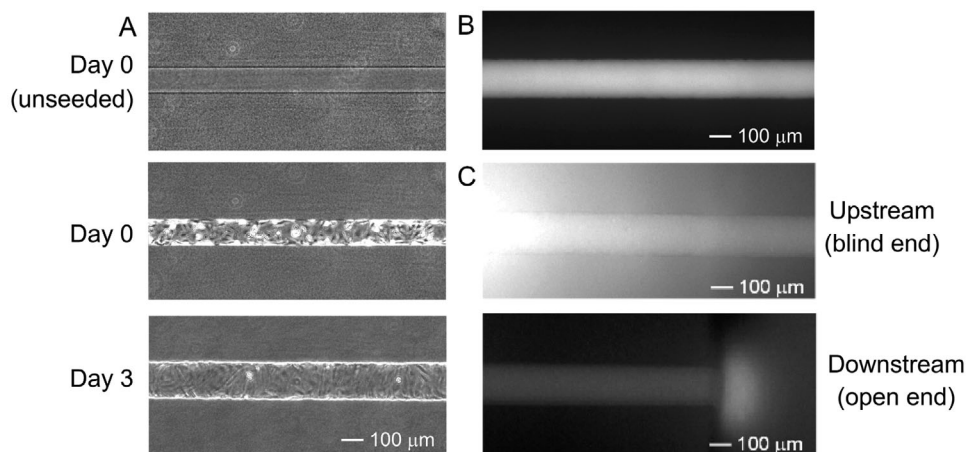


Figure 5. Microfluidic vascularization. A) Time-lapse images of a microfluidic collagen gel and the growth of a vessel within the channel. Adapted with permission.^[62] Copyright 2011, Springer Nature. B) Fluorescence image of an engineered microvessel after perfusion with fluorescently labeled albumin. Restriction of solute to the lumen indicates a strong barrier. Adapted with permission.^[62] Copyright 2011, Springer Nature. C) Fluorescence image of an engineered lymphatic after introduction of fluorescent 10 kDa dextran to the collagen gel near the blind end (top). Solute is transported into the lymphatic and drains from it at the open end (bottom). Adapted with permission.^[17] Copyright 2018, Wiley.

is monolithic. As predicted theoretically,^[60] the applied pressure controls the diameter of the resulting channel (more precisely, the ratio of the channel diameter to PDMS chamber width).^[59]

The disadvantage of viscous fingering is that it lacks geometric versatility. Each feature of the PDMS chamber will contain one, and only one, channel. The width of the channel is 50–80% of that of the PDMS chamber; thinner channels have not been reported for the applied pressures and precursor viscosities used.^[23,59] In these microfluidic biomaterials, the channel occupies a substantial volume fraction (25–65%) of the total material. Also, it is not clear whether large-scale microfluidic networks can be made with viscous fingering. Nevertheless, for applications in which having any microfluidic geometry—regardless of the channel size or interconnectivity—is sufficient, viscous fingering offers a simple and elegant alternative to the approaches based on molding or printing.

2.4.2. Other Approaches

Electric discharge has been used to create fractal vessel-like networks in a degradable polymer.^[61] This approach is remarkable in its ability to generate large 3D branching networks in one step, albeit at the cost of variability in the network geometry.

3. Microfluidic Biomaterials as Scaffolds for Microvascular and Epithelial Tissue Engineering

The original motivation for the development of microfluidic biomaterials, and their most important application to date, is the creation of perfusable scaffolds for engineering tissues. All tissues require some level of flow and/or exchange of fluids and solutes for proper function. In most tissues, the most important features that mediate this transport are the blood and lymphatic vascular networks that provide nutrients and drainage, respectively. Other networks include the airway system in the lung for transport of

oxygen and carbon dioxide, the tubular and collecting systems in the kidney for transport of renal filtrate and urine, and the ductal trees in exocrine glands for transport of glandular secretions. The ability to build biomaterials that contain microfluidic networks with geometries similar to native biological transport networks has motivated the application of these materials to tissue engineering.

To date, these applications have mainly been used in microphysiological systems, for the modeling of human physiology or dysfunction in microscale tissues. Applications to regenerative medicine are more speculative at this point.

3.1. Microfluidic Vascularization

By far, the most important driver for the development of microfluidic biomaterials has been to create a scaffold that is designed specifically to promote vascularization (Figure 5A).^[10,11] Prior to the development of these materials, methods to vascularize scaffolds relied exclusively on mimicking the natural biological processes of angiogenesis (vascular sprouting) or vasculogenesis (formation of vascular networks from individual cells).^[11] Since these biological processes are defined by the intrinsic morphogenetic movements of vascular cells, they are slow and provide poor control over the resulting vascular geometries.

Compared to angiogenic or vasculogenic approaches, vascularization via the use of microfluidic biomaterials (so-called “microfluidic vascularization”) provides several advantages. First, the ability to immediately perfuse the materials means that any cells in the bulk region can be fed without delay. Second, the channels serve as templates to control where the vessels form, and the vessel geometries are defined by the user. Tissues with nearly identical vessel geometries can be made with microfluidic biomaterials, which can be useful if one wishes to study vessel–tissue interactions without confounding variations in vascular geometry. Disjoint microfluidic patterns can be used to engineer separate vascular and lymphatic networks within the same scaffold.

Third, the precise vascular geometry afforded by microfluidic biomaterials enables the use of computational design to optimize the geometry for a desired transport or drainage function.

For channels wider than $\approx 30\ \mu\text{m}$, vascularization proceeds by flowing a dense suspension of endothelial cells into the channels. Because the size of a cell is smaller than the channel width, the cells will distribute throughout the network. As long as the biomaterial is naturally adhesive to cells (e.g., type I collagen, fibrin), the cells will adhere, spread, and eventually grow to form a confluent lining. For nonadhesive materials (e.g., gels of PEG, agarose, or dextran), covalent coupling of adhesive peptides or entangling of matrix proteins is sufficient to enable formation of a confluent endothelial tube.^[15,41,63] Vascularization by direct seeding has been successfully demonstrated in single channels and entire networks.^[12,34,38] With care to avoid excess cell accumulation, it can be applied to blind-ended channels as well.^[17] Flow is maintained in these scaffolds by establishing a hydrostatic pressure difference across the ends of a channel or by using pump-driven flow.

For channels narrower than $\approx 30\ \mu\text{m}$, direct seeding results in plugging of the channels. As a result, the cells are not initially well-distributed through channels of this size. Vascularization thus requires that the seeded cells migrate along the walls of the channel, which can be promoted with physical and/or chemical signals.^[26] It is also possible to use selective ablation of endothelial cells with a laser to promote migration of the remaining intact cells along a capillary-scale channel.^[48]

A different strategy for microfluidic vascularization is to embed endothelial cells within a sacrificial rod or mesh before molding a biomaterial around it. This approach has been demonstrated with 3D-printing of sacrificial gelatin structures.^[55,64] Once encapsulated in a collagen gel, the gelatin can be melted to release the endothelial cells, which then adhere to the resulting channels. A related strategy uses electrochemical transfer of endothelial cells from a rod to the surrounding material, before removal of the rod.^[65,66]

3.1.1. Vascular Stability and Function in Microfluidic Biomaterials

Although the channels in microfluidic biomaterials can serve as templates for the formation of perfused microvessels, they do not guarantee that these vessels will be stable over the long term, or that the vessels will be functional. Important microvascular functions include: the generation of a barrier between the intra- and extravascular space, maintenance of blood fluidity, oxygenation of the surrounding tissue, autoregulation of blood flow, control of the local inflammatory response, hormone processing, and tissue drainage.^[67] For these functions to be present in an engineered tissue, at minimum the vessels must not regress over the long term.

The ability to control vascular geometry and perfusion conditions within microfluidic biomaterials has enabled the elucidation of signals that govern vascular stability in these materials. In particular, vascular stability appears to be a mechanical phenomenon.^[68] Stable vasculature requires that the mechanical stress at the interface between endothelial cells and the surface of the biomaterial channel be sufficiently small. Signals that decrease this stress, whether directly (such as high perfusion

pressure^[69] and low scaffold pressure^[29]) or indirectly (such as tightening the vascular barrier with analogs of cyclic AMP^[70] or crosslinking the scaffold^[71]), improve vascular stability. Under optimized conditions, the vessels within microfluidic scaffolds can be perfused for over 2 months. In the absence of sufficient stabilizing signals, the endothelial cells can detach as single cells or delaminate as multicellular patches from the biomaterial.

Generating stable blind-ended lymphatic vessels has been more challenging. Drainage function requires the extravascular pressure to exceed the intravascular one, a situation that is mechanically destabilizing. Indeed, even under optimized conditions, the endothelium in these vessels begins to delaminate if the scaffold pressure exceeds vascular pressure for more than a few hours.^[17] In vivo, the lymphatic endothelium is tethered to the surrounding tissue by fibrillin-rich anchoring filaments.^[72] Perhaps the incorporation of fibrillin into the collagen gel, either throughout the bulk or only at the surface of the channel, would aid in the preservation of lymphatic stability under physiological conditions.

Of all the microvascular functions, barrier function is the one that is most assayed in microfluidic vascularization (Figure 5B). Assessment of barrier function consists of quantifying the ability of the vascular wall to restrict the passage of solutes between the perfusate and the biomaterial bulk. Although it may seem counterintuitive (after all, the purpose of the microfluidic network is to increase the rate of transport), the emergence of a physiological barrier is important to obtain the proper solute concentrations and fluid flows within the biomaterial bulk. The endothelial barrier serves to shield any cells in the biomaterial from inappropriate levels of interstitial flow. In vivo, the tightness of the microvascular barrier ranges from extreme impermeability in the brain to extreme porosity in the liver.^[73] Microvessels for most tissues (e.g., skin, heart, adipose) lie somewhere in the middle in their barrier function and are considered “continuous.” The appropriate barrier function for engineered microvessels should be analyzed with the relevant tissue in mind.

Quantification of barrier function relies on measuring the permeability coefficients to various fluorescently labeled solutes, such as serum albumin and dextrans. For models of the blood-brain barrier (BBB), the fluorescent solutes used for permeability measurements are much smaller in molecular weight.^[74] Permeability coefficients treat the vessel wall as a uniformly permeable membrane and provide an average measure of the vessel leakiness. Alternatively, barrier function can be assessed by counting the number of “focal” leaks along the vessel walls. In principle, the permeability coefficients and focal leak densities that are measured for engineered microvessels can be directly compared to the equivalent values reported in vivo. To date, a much wider range of values has been reported for engineered, compared to physiological, microvessels. This disparity stems both from differences in the perfusion conditions that are applied in different studies of vascularized biomaterials and from differences in how the permeability assays are performed. Detailed protocols for measuring permeability coefficients, including the required control experiments, are available.^[62]

Strong barrier function is fostered by many of the same signals that promote vascular stability, such as high flow and elevation of intracellular cyclic AMP levels.^[69,70,75] Under optimized conditions, the permeability values fall in the same range as those

reported *in vivo* for continuous endothelium. Even for more specialized barriers, such as the unusually tight BBB, perfusion-derived signals appear to be sufficient to generate the desired level of barrier function.^[74] Although signals from support cells, such as astrocytes and pericytes, that are embedded within the surrounding tissue are important to maintain the BBB *in vivo*, a BBB-like barrier can be obtained *in vitro* without the addition of these nonvascular cells. Microvessels that are formed from kidney microvascular endothelial cells do *not* form a tight barrier, and instead display a leaky fenestrated endothelium that is characteristic of renal peritubular capillaries.^[76] Similarly, vessels of tumor-derived endothelial cells are prone to intercellular gaps and spontaneous sprouting.^[77] The relative importance of cell-autonomous and microenvironmental conditions in controlling barrier function in vascularized microfluidic biomaterials requires further investigation.

Microvessels within microfluidic biomaterials have been used as microphysiological systems to analyze microvascular behavior in the presence of perfusion. For instance, they have provided insight in the molecular mechanisms that govern vascular barrier function and its breakdown and flow-induced angiogenesis.^[78–81] Vessels that are formed adjacent to an empty channel that delivers angiogenic factors have been used to probe the mechanisms of vascular endothelial growth factor (VEGF)- and geometry-dependent angiogenesis under perfusion.^[30,82,83] Vessels that are formed from induced pluripotent stem cell (iPSC)-derived brain microvascular endothelial cells have been used to elucidate the mechanisms of hyperosmotic BBB opening.^[84] Perfused microvascular networks have been used to test the effects of ultrasound on delivery of solutes to the vascular wall via sonoporation.^[85] The behavior of endothelial cells in these perfusable vessels can differ substantially from that in other 3D and 2D culture formats.^[77,86]

Similar approaches can be used to analyze vascular activation during inflammation and thrombosis. In general, signals that inflame vessels *in vivo* do the same *in vitro*, and engineered microvessels can be tuned to display a low baseline level of activation.^[12,38] Upon treatment with inflammatory signals, the endothelium can support the adhesion of leukocytes and platelets and the transmigration of leukocytes, as observed *in vivo*.^[12,38,87] Perfusion with platelet-rich plasma results in the formation of a plug when a segment of the endothelium is injured.^[88] Vascularized capillary-scale channels have found particular use in the analysis of vascular occlusion, which is a primary consequence of sickle cell disease and malaria. Malaria-infected erythrocytes can occlude engineered microvessels and cause a transient increase in vascular permeability.^[41,48]

Blind-ended channels can be used to form blind-ended vessels that serve as artificial lymphatics. These vessels are intended to drain the biomaterial of excess solutes and fluid. A systematic comparison of unseeded and seeded blind-ended channels in their drainage ability has shed light on the design principles that govern effective drainage.^[17] As expected, the presence of a channel increases the drainage rate over that of a solid gel. The presence of endothelium in the channel does not alter the rate of fluid drainage over that achievable with an unseeded channel. Surprisingly, the presence of endothelium *increases* the rate of solute drainage over that of an unseeded channel. The endothelium appears to have segmental properties: at the blind end (i.e., lym-

phatic tip), the endothelium is leaky and allows entry of fluid and solutes into the vessel; downstream, the endothelium is tight and does not allow escape back into the surrounding scaffold (Figure 5C). This mechanism of drainage mimics that of native lymphatics *in vivo*.

3.1.2. Generation of Vascularized Tissues in Microfluidic Biomaterials

In conjunction with microfluidic vascularization, inclusion of nonvascular cells within the biomaterial bulk can be used to generate vascularized tissues. To date, these tissues have been small-scale analogs that are better suited for microphysiological systems than for regenerative medicine. Given the emphasis on generating microvessels with a strong barrier, it is perhaps not surprising that the tissues examined to date have consisted mainly of those with continuous vessels, such as adipose, skin, and myocardium.

Vascularized adipose in microfluidic collagen gels can be engineered by embedding adipocytes within the gel (Figure 6A).^[89] The resulting tissue responds appropriately to perfusion with lipogenic or lipolytic hormones by expansion or shrinkage of the lipid droplets, respectively. The presence of adipocytes leads to a modest increase in vascular permeability. The microscale vascularized adipose tissues are envisioned for studies of vessel-adipocyte interactions during obesity and other metabolic conditions.

Similar approaches have been used to create vascularized models of bone marrow and liver.^[49,90] Here, the collagen gels contain bone marrow aspirate, purified megakaryocytes (cells that produce platelets), or hepatocytes. The presence of megakaryocytes induces micrometer-sized holes within the vascular layer, and transforms the vessel from a continuous to a discontinuous one similar to bone marrow microvessels. Although applied for the study of thrombopoiesis, these vascularized bone marrow tissues could find broader use for modeling other vascular processes in the marrow, such as the egress and homing of marrow-derived stem and progenitor cells. Vascularized liver tissue produces more urea per hepatocyte than a standard 3D bulk or sandwich culture does, and has been used to investigate drug hepatotoxicity.^[13,49,91]

Vascularized skin equivalents consist of epidermal keratinocytes that are seeded on top of a vascularized microfluidic gel that contains dermal fibroblasts (Figure 6B).^[64,92,93] These constructs display appropriate barrier function, as shown by capacitance measurements in dermal and epidermal layers. The epidermal layer can mature sufficiently to repel applied water droplets. Measurements of percutaneous absorption using two drugs (caffeine and isosorbide dinitrate) have been used to test the physiological relevance of these constructs. The skin equivalents are intended as alternatives to whole-animal tests of vascular irritancy and as vascularized skin grafts.

In contrast to adipose and skin, myocardium is mechanically active, and attention must be paid to the cell-induced deformation of the biomaterial. Vascular and myocardial tissue functions appear to be antagonistic: the formation of mature myocardium is favored by low-density (1.25 mg mL⁻¹) collagen, but such dilute gels are too weak to support the formation of a perfusable

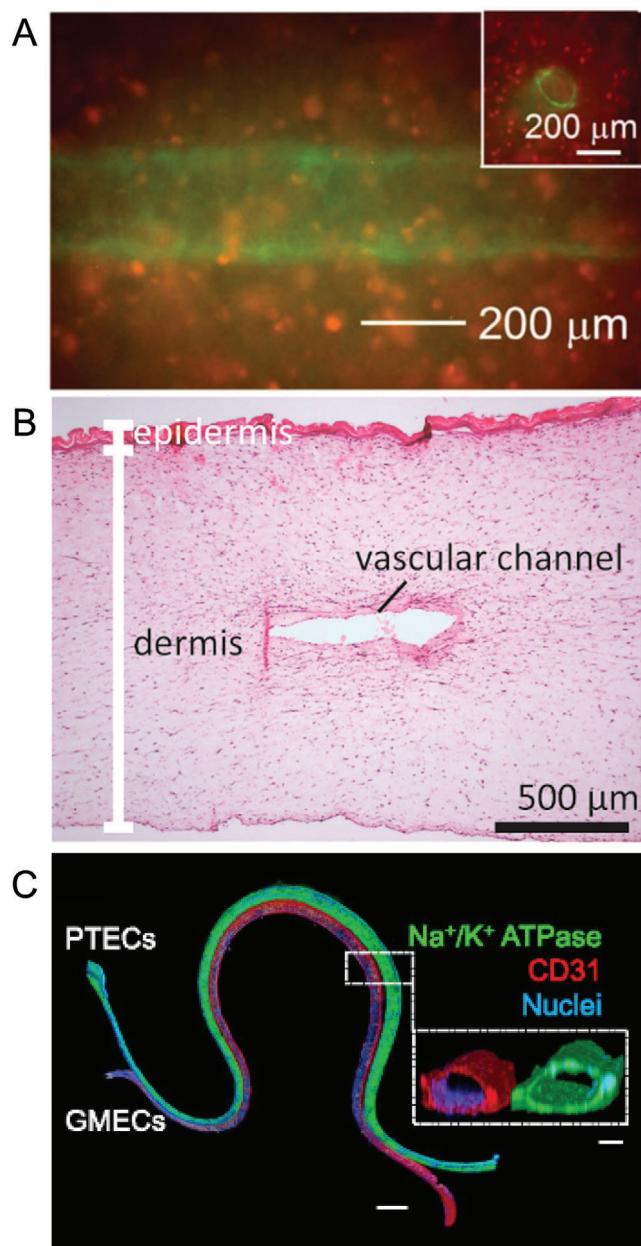


Figure 6. Microfluidic vascularization. A) Vascularized adipose tissue after 3 days of perfusion, stained for endothelial cell marker CD31 (green) and neutral lipids (red). Reproduced with permission.^[89] Copyright 2019, IOP Publishing. B) Vascularized skin equivalent. Reproduced with permission.^[92] Copyright 2017, Elsevier. C) Vascularized proximal tubule in 3D-printed channels, stained for CD31 (red), epithelial cell marker Na^+/K^+ -ATPase (green), and DNA (blue). Scale bars refer to 1 mm (main image) and 100 μm (inset). Adapted with permission.^[94] Copyright 2019, National Academy of Sciences.

microvascular network. When embedded within microfluidic high-density (6 mg mL^{-1}) collagen gels that contain a molded vascular network, embryonic stem cell (ESC)-derived cardiomyocytes mature to form anisotropic tissues only in the presence of co-cultured stromal cells in the gel bulk.^[95] The addition of stromal cells to high-density gels enables the matrix remodeling

that is required for embedded cardiomyocytes to reorganize into mature structures.

Vascularized renal tissue has been constructed with microfluidic fibrin-gelatin gels, in which separate serpentine channels for endothelial and proximal tubular epithelial cells are printed via a subtractive ink (Figure 6C).^[94] When seeded with their respective cell types, these channels mature into intertwined vessel and proximal tubule, both of which can be independently perfused. This tissue is able to mimic kidney filtration and reabsorption of solutes from tubular to vascular lumen. Reabsorption of albumin and glucose has been used to demonstrate renal functionality. Hyperglycemic perfusion of the proximal tubule results in endothelial injury that is ameliorated with an inhibitor of tubular glucose transport. Layered vascular and tubular networks, generated from micromolded networks in a collagen gel, also demonstrate kidney-specific reabsorption.^[96]

Vascularized tumors have been formed to study tumor progression and tumor-induced angiogenesis under perfused conditions. The simplest configuration is to embed tumor cells individually or as aggregates within the biomaterial that contains a vessel. This setup has been used with breast cancer cells or their associated fibroblasts to analyze how they intravasate into the vascular lumen under flow and how they influence lymphatic function.^[97–100] These tumors have also enabled the vascular delivery, extravasation, and migration of natural killer cells to the embedded tumor cells.^[101] A similar system with patient-derived renal carcinoma cells around a perfused vessel results in angiogenesis that is mediated by soluble VEGF.^[102] A more elaborate system uses two separate channels to localize a tube or packed aggregate of tumor cells near a perfusable vessel. This setup has been used to study the induction of lymphangiogenesis by breast cancer cells^[103] and the progression of pancreatic and breast micro-tumors from confined growth to intravasation into a neighboring vessel (Tien and Dance, unpublished data).^[100,104]

When embedding or printing nonvascular cells within the biomaterial bulk of microfluidic scaffolds to generate perfusable tissues, it is important to ensure that the patterning technique is compatible with the desired combination of cell type and biomaterial composition. For instance, microfluidic channels can be more easily molded into biomaterials that are more concentrated, but the smaller pore size in such concentrated materials can limit the viability of embedded cells. Also, 3D-printing of cell-laden inks can result in loss of cell viability as a result of excessive printing-induced stresses. Given the diversity of available strategies for generating microfluidic biomaterials, it is often possible to find at least one suitable method for a given cell type and biomaterial.

Although the physiological condition is a sustained and pulsatile vascular flow, not all studies have actually maintained perfusion during the maturation of the tissue.^[89,92,94,97,102] In many cases, perfusion was transient and episodic, with a large initial flow rate followed by rapid decay of the flow as the driving pressure difference dissipated.^[90,95] Whether the transient versus sustained nature of the perfusion alters the function of these engineered tissues or of the vessels that they contain remains to be clarified.

In the few studies that have reported in vivo grafting of vascularized microfluidic scaffolds, perfusion through the preformed vessels was often not maintained after grafting.^[64,105,106]

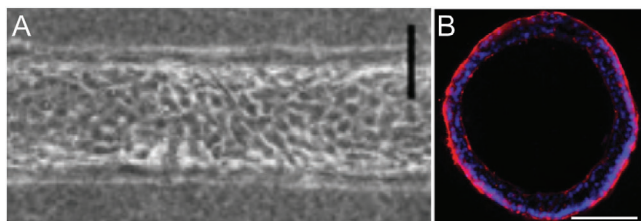


Figure 7. Microfluidic epithelialization. A) Perfusable renal proximal epithelial tube. Scale bar refers to 50 μm . Adapted with permission.^[109] Copyright 2016, Elsevier. B) Perfusable MCF7 mammary epithelial tube, stained for F-actin (red) and DNA (blue). Scale bar refers to 100 μm . Adapted with permission.^[113] Copyright 2018, Springer Nature. Compared to the thin endothelial lining in Figure 5A, the epithelium forms a noticeably thicker layer in both tubes.

Although the vessels persist in the graft, much of the perfusion into the graft derives from vascular ingrowth from the host, rather than from flow through the vascularized microchannels.^[106] The implanted microchannels can also guide the growth of new vessels from the host.^[64] Nevertheless, these studies have shown that the presence of the implanted vessels results in enhanced delivery of oxygen to a tissue after grafting and to host tissue distal to the graft.^[105,106] As has been observed in other types of grafts,^[107] the therapeutic benefit from vascularized microfluidic scaffolds appears to stem in large part from paracrine effects, rather than from the persistent incorporation of grafted cells. Direct, cuff-based surgical anastomosis of host vessels to a polymer-based microfluidic scaffold has been shown to result in sustained perfusion after grafting, even if the channels are not initially vascularized.^[49]

3.2. Microfluidic Epithelialization

Although originally intended for engineering microvasculature, the tubular geometry of channels within microfluidic biomaterials has also been used recently to engineer epithelial tubes and ducts. One example is the renal tubule: immortalized (Madin-Darby canine kidney, MDCK) renal epithelial cells can grow to form functional epithelial tubes in microfluidic collagen gels that are formed with rod-based molding.^[108] These tubes display an extremely tight barrier that is typical of epithelium and brain microvessels. Subsequent studies have used primary human proximal tubule epithelial cells to form the tubules, with rod-based molding or 3D-printed sacrificial channels (Figure 7A).^[109–111] These structures display glucose reabsorption and metabolic abilities that are consistent with proximal tubules *in vivo*.^[109] Given

that many nephrotoxic drugs exert their effect on the proximal tubule, the engineered tubules have been used for nephrotoxicity drug screening, with expression of heme oxygenase-1 as the primary toxicity marker.^[110] Coupling the input of the perfused tubule to the output of a liver-on-a-chip device provides a tool for studying the role of liver-induced bioactivation in generating nephrotoxins.^[112]

Breast epithelial ducts have been formed in microfluidic collagen gels that are formed with viscous fingering or rod-based methods (Figure 7B).^[113,114] These ducts can be back-filled with genetically abnormal breast epithelial cells to mimic carcinoma *in situ*, a condition that is believed to be the precursor to invasive breast carcinoma.^[114,115] These models have been made even more elaborate with the inclusion of fibroblasts or adipose stromal cells in the gel.^[113,115,116] Epithelial cell behavior in 3D engineered ducts can be strikingly different from that in nonductal 3D cultures (i.e., cells embedded in a gel) or in planar 2D cultures.^[86] Blind-ended channels can be filled with breast cancer cells to form micro-tumors that invade under flow.^[16]

Other types of epithelial tubes are less commonly studied. Recent work has reported the use of a multi-channeled microfluidic collagen/fibrinogen gel to engineer an open small-diameter bronchiole flanked by perfusable vessels.^[117] This system was used to examine the interaction of microbes in the airway with leukocytes in the vascular lumens.

4. Microfluidic Biomaterials as Guides for Transport and Growth

Even when they are not lined with endothelial or epithelial cells, the built-in channels in microfluidic biomaterials render these materials well-suited to the delivery and/or removal of solutes. Thus, it is possible to use the channels purely as conduits for convective flow of a desired aqueous solution, independent of any cell lining. Alternatively, the channels can serve as passive guides to direct tissue growth.

4.1. Tissue Engineering

When the scaffold bulk contains embedded cells, perfusion of unlined microfluidic channels can be used to deliver nutrients and remove metabolites from the cells (Figure 8).^[9,39,118] This approach to tissue engineering treats the microfluidic scaffold as a bioreactor, through which fluids can be pumped. The well-defined geometries of the perfused channels has helped to elucidate the basic principles of solute delivery in microfluidic biomaterials. The major concept is that of the Krogh radius, the furthest

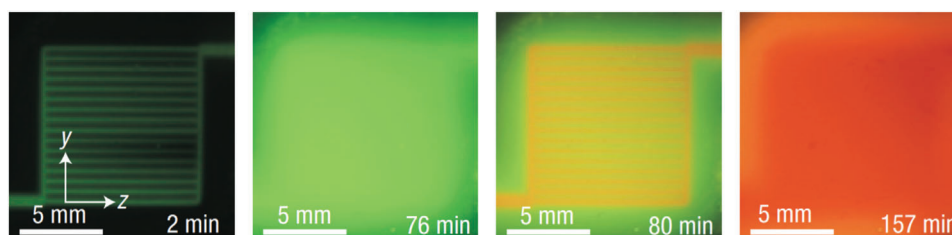


Figure 8. Use of microfluidic biomaterials as transport networks. Sequential perfusion of a microfluidic alginate gel with fluorescein- and rhodamine-containing solutions leads to delivery and removal of the solutes. Reproduced with permission.^[9] Copyright 2007, Springer Nature.

distance from a channel wall to which solutes can be functionally delivered.^[9,50] As predicted by scaling analysis, this distance λ depends on the solute consumption rate R_0 per cell, the density ρ of embedded cells, the solute concentration C_0 at the inlet of the channels, and the solute diffusivity D within the scaffold^[9]

$$\lambda \sim \sqrt{\frac{DC_0}{\rho R_0}}$$

A similar expression holds in tissues that are formed with microfluidic vascularization, as shown with vascularized adipose.^[89] The idea of a Krogh radius has been tested with cell-laden gels that contain individual chondrocytes.^[9] The further the embedded cells are from the channel, the less metabolically functional they are. When the bulk contains individual endothelial cells, these cells can migrate to the surface of a channel and eventually vascularize them.^[119]

4.2. Wound Healing

When applied to a wound, a microfluidic biomaterial can serve as an acellular bandage or wound dressing (Figure 9A).^[7,120] Unlike a passive dressing such as gauze, here the biomaterial can alter the wound fluid by having a perfusate pumped into the dressing. Although this concept has yet to be implemented in a microfluidic design, the basic capabilities have been demonstrated in the hydrogel poly(hydroxyethyl methacrylate) (pHEMA). This material can be photopatterned into regions of different pore size,^[7] and pressure-driven flow across a layer of pHEMA can deliver solutes to an underlying substrate.^[120] The open question is whether the ability to control the wound milieu justifies the extra cost and difficulty of fabrication. Competing techniques, such as negative-pressure wound therapy, are not as versatile as a microfluidic dressing, but may be sufficient to reap most of the benefits from conditioning the wound fluid. Perhaps the ability of a microfluidic dressing to deliver growth factors at defined locations and during different stages of wound healing would help accelerate tissue regeneration.

An unrelated use of microfluidic biomaterials in wound healing is to direct the ingrowth of vascularized connective tissue (Figure 9B).^[121] The channels serve as guides for ingrowth, and can also be filled with dilute collagen gel to provide a sparse provisional matrix for cell migration. Surprisingly, tissue ingrowth into channels that are pre-filled with dilute collagen is comparable to that into unfilled channels.

5. Computational Design of Microfluidic Biomaterials

To date, the study of microfluidic biomaterials has been heavily experimental. Nevertheless, the precise geometries of microfluidic biomaterials render them amenable to computational modeling and optimization, and some studies have applied analytical and finite-element approaches to microfluidic design. Two types of fluidic geometries are most commonly modeled: parallel arrays of channels, and branching networks. Model parallel arrays have been used to determine the optimal channel spacing

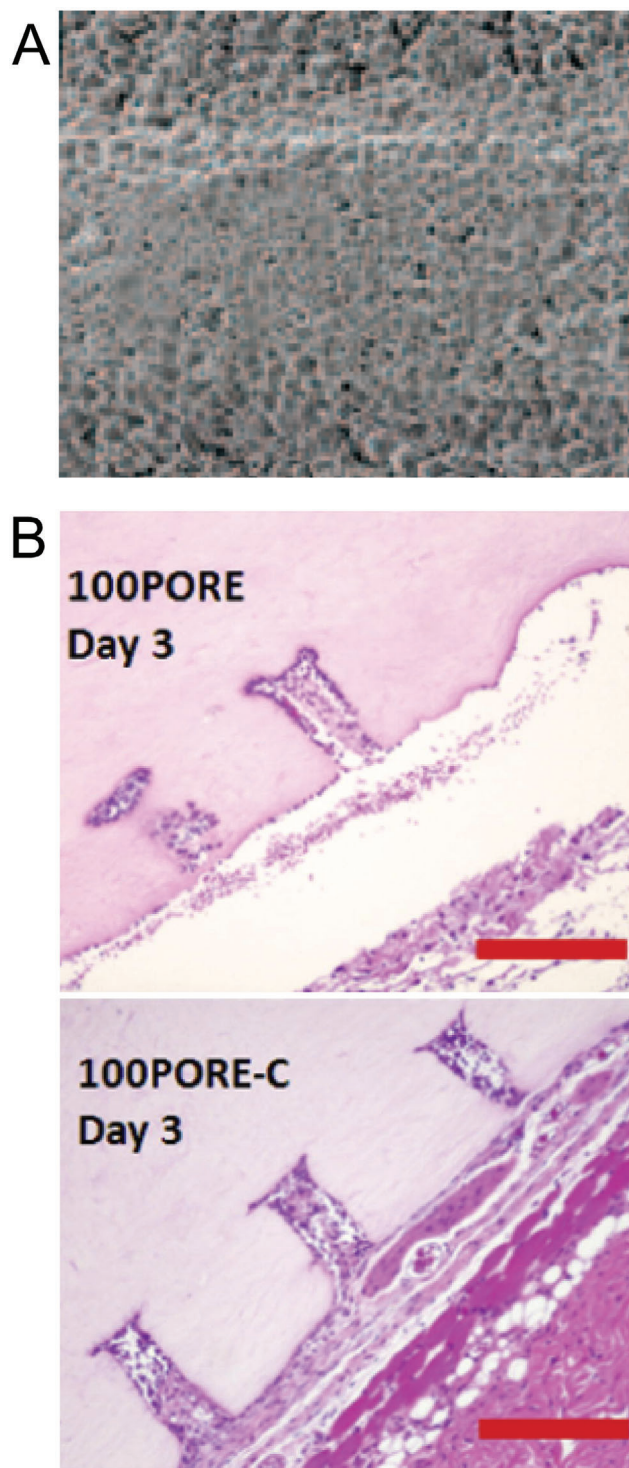


Figure 9. Use of microfluidic biomaterials in wound healing. A) Scanning electron micrograph of a porous microfluidic pHEMA sponge that is photopatterned to contain a 1 mm wide region of different pore structure. Such materials have been proposed as the main element in active wound dressings. Adapted with permission.^[7] Copyright 2006, Cambridge University Press. B) Microfluidic collagen gels (20 mg mL^{-1}) after subcutaneous grafting in mice. Channels in the gels were either unfilled (top) or backfilled with dilute (3 mg mL^{-1}) collagen (bottom) before implantation. Scale bars refer to $200 \mu\text{m}$. Adapted with permission.^[121] Copyright 2011, Elsevier.

to obtain sufficient oxygen delivery and vascular stability within microfluidic biomaterials.^[118,122,123] Model branching networks have been used to determine the optimal branching ratios needed to minimize pumping power without compromising transport rate.^[124] Not surprisingly, these geometries resemble those of native biological transport networks, particularly in their adherence to Murray's law, which relates the channel diameters at a junction in the network.

When optimizing microfluidic design, it is important to state explicitly what parameter is being maximized or minimized and what constraints are applied. For example, a network to deliver nutrients to all cells in the scaffold while minimizing channel surface area will have a different geometry than one that minimizes the vascular volume.^[125] Despite the potential of computational modeling, such approaches have been used primarily to analyze transport in a given microfluidic geometry, rather than to optimize the design for a desired output. As a result, the selection of microfluidic geometry still remains driven more by intuition than by computation, and much more work is needed to realize the potential of computational tools for rational design of these materials.

6. Conclusions and Future Directions

Since their invention in 2005, microfluidic biomaterials have generated tremendous interest in the biomaterials and tissue engineering communities. Their use in microfluidic vascularization has shown clear advantages over techniques that rely on biological vascular morphogenesis, such as angiogenesis and vasculogenesis. Recent work has also begun to exploit the capability of microfluidic biomaterials to template the formation of perfusable epithelial tubes. Other applications that treat the microfluidic features solely as a delivery network for solutes or fluids have reached the proof-of-concept stage.

It is highly likely that the coupling of vascular and epithelial structures into a single biomaterial, especially with the further refinement of 3D printing, will continue. The incorporation of capillary-scale channels, organ-specific vascular geometries, and/or patient-derived cells will enable microphysiological systems to approximate native tissue organization more closely. For applications in regenerative medicine, whether the unique capabilities of microfluidic biomaterials are sufficient to justify the extra complexity of scaffold synthesis remains to be seen. Nevertheless, the progress that has been achieved in the last 15 years is heartening, and it is a solid bet that future studies will develop new applications that have yet to be envisioned.

Acknowledgements

The authors thank Alex Seibel for providing helpful comments. This review is dedicated to Prof. George Whitesides, who is the academic "father" of J.T. and "grandfather" of Y.W.D. The authors hope that this review provides a window into one field of materials research in which former members of the Whitesides Group have been, and continue to be, key contributors. Support during the preparation of this article was provided by the National Cancer Institute through award CA214292, the National Institute of General Medical Sciences (Grant No. T32 GM008764) and the CURE Diversity Research Supplements Program.

Conflict of Interest

The authors declare no conflict of interest.

Keywords

collagen, hydrogels, microphysiological systems, microvascular tissue engineering, perfusion

Received: June 17, 2020

Revised: August 15, 2020

Published online: September 6, 2020

- [1] G. M. Whitesides, *Nature* **2006**, 442, 368.
- [2] E. K. Sackmann, A. L. Fulton, D. J. Beebe, *Nature* **2014**, 507, 181.
- [3] D. J. Beebe, G. A. Mensing, G. M. Walker, *Annu. Rev. Biomed. Eng.* **2002**, 4, 261.
- [4] H. A. Stone, A. D. Stroock, A. Ajdari, *Annu. Rev. Fluid Mech.* **2004**, 36, 381.
- [5] Y. Yang, K. Gupta, K. L. Ekinici, *Proc. Natl. Acad. Sci. U. S. A.* **2020**, 117, 10639.
- [6] A. W. Martinez, S. T. Phillips, B. J. Wiley, M. Gupta, G. M. Whitesides, *Lab Chip* **2008**, 8, 2146.
- [7] A. D. Stroock, M. Cabodi, *MRS Bull.* **2006**, 31, 114.
- [8] M. Cabodi, N. W. Choi, J. P. Gleghorn, C. S. Lee, L. J. Bonassar, A. D. Stroock, *J. Am. Chem. Soc.* **2005**, 127, 13788.
- [9] N. W. Choi, M. Cabodi, B. Held, J. P. Gleghorn, L. J. Bonassar, A. D. Stroock, *Nat. Mater.* **2007**, 6, 908.
- [10] J. Tien, *Curr. Opin. Chem. Eng.* **2014**, 3, 36.
- [11] J. Tien, *Compr. Physiol.* **2019**, 9, 1155.
- [12] K. M. Chrobak, D. R. Potter, J. Tien, *Microvasc. Res.* **2006**, 71, 185.
- [13] J. S. Miller, K. R. Stevens, M. T. Yang, B. M. Baker, D.-H. T. Nguyen, D. M. Cohen, E. Toro, A. A. Chen, P. A. Galie, X. Yu, R. Chaturvedi, S. N. Bhatia, C. S. Chen, *Nat. Mater.* **2012**, 11, 768.
- [14] D. B. Kolesky, R. L. Truby, A. S. Gladman, T. A. Busbee, K. A. Homan, J. A. Lewis, *Adv. Mater.* **2014**, 26, 3124.
- [15] K. A. Heintz, M. E. Bregenzler, J. L. Mantle, K. H. Lee, J. L. West, J. H. Slater, *Adv. Healthcare Mater.* **2016**, 5, 2153.
- [16] J. Tien, J. G. Truslow, C. M. Nelson, *PLoS One* **2012**, 7, e45191.
- [17] R. L. Thompson, E. A. Margolis, T. J. Ryan, B. J. Coisman, G. M. Price, K. H. K. Wong, J. Tien, *J. Biomed. Mater. Res., Part A* **2018**, 106, 106.
- [18] S. F. Badylak, D. Taylor, K. Uygun, *Annu. Rev. Biomed. Eng.* **2011**, 13, 27.
- [19] J. Huling, I. K. Ko, A. Atala, J. J. Yoo, *Acta Biomater.* **2016**, 32, 190.
- [20] J. R. Gershlak, S. Hernandez, G. Fontana, L. R. Perreault, K. J. Hansen, S. A. Larson, B. Y. K. Binder, D. M. Dolivo, T. Yang, T. Dominko, M. W. Rolle, P. J. Weathers, F. Medina-Bolivar, C. L. Cramer, W. L. Murphy, G. R. Gaudette, *Biomaterials* **2017**, 125, 13.
- [21] K. H. Benam, S. Dauth, B. Hassell, A. Herland, A. Jain, K.-J. Jang, K. Karalis, H. J. Kim, L. MacQueen, R. Mahmoodian, S. Musah, Y. Torisawa, A. D. van der Meer, R. Villenave, M. Yadid, K. K. Parker, D. E. Ingber, *Annu. Rev. Pathol.: Mech. Dis.* **2015**, 10, 195.
- [22] Y. I. Wang, C. Carmona, J. J. Hickman, M. L. Shuler, *Adv. Healthcare Mater.* **2018**, 7, 1701000.
- [23] L. L. Bischel, S.-H. Lee, D. J. Beebe, *J. Lab. Autom.* **2012**, 17, 96.
- [24] Y. N. Xia, J. J. McClelland, R. Gupta, D. Qin, X. M. Zhao, L. L. Sohn, R. J. Celotta, G. M. Whitesides, *Adv. Mater.* **1997**, 9, 147.
- [25] G. M. Price, J. Tien, in *Microdevices in Biology and Engineering* (Eds: S. N. Bhatia, Y. Nahmias), Artech House, Boston, MA **2009**, p. 235.
- [26] R. M. Linville, N. F. Boland, G. Covarrubias, G. M. Price, J. Tien, *Cell. Mol. Bioeng.* **2016**, 9, 73.

- [27] J. A. Jiménez-Torres, S. L. Peery, K. E. Sung, D. J. Beebe, *Adv. Healthcare Mater.* **2016**, *5*, 198.
- [28] M. D. Tang, A. P. Golden, J. Tien, *J. Am. Chem. Soc.* **2003**, *125*, 12988.
- [29] K. H. K. Wong, J. G. Truslow, A. H. Khankhel, K. L. S. Chan, J. Tien, *J. Biomed. Mater. Res., Part A* **2013**, *101A*, 2181.
- [30] D.-H. T. Nguyen, S. C. Stapleton, M. T. Yang, S. S. Cha, C. K. Choi, P. A. Galie, C. S. Chen, *Proc. Natl. Acad. Sci. U. S. A.* **2013**, *110*, 6712.
- [31] J. W. Nichol, S. T. Koshy, H. Bae, C. M. Hwang, S. Yamanlar, A. Khademhosseini, *Biomaterials* **2010**, *31*, 5536.
- [32] W. Zhang, L. S. Wray, J. Rnjak-Kovacina, L. Xu, D. Zou, S. Wang, M. Zhang, J. Dong, G. Li, D. L. Kaplan, X. Jiang, *Biomaterials* **2015**, *56*, 68.
- [33] L. E. Bertassoni, M. Cecconi, V. Manoharan, M. Nikkhah, J. Hjortnaes, A. L. Cristino, G. Barabaschi, D. Demarchi, M. R. Dokmeci, Y. Yang, A. Khademhosseini, *Lab Chip* **2014**, *14*, 2202.
- [34] A. P. Golden, J. Tien, *Lab Chip* **2007**, *7*, 720.
- [35] S. Zhao, Y. Chen, B. P. Partlow, A. S. Golding, P. Tseng, J. Coburn, M. B. Applegate, J. E. Moreau, F. G. Omenetto, D. L. Kaplan, *Biomaterials* **2016**, *93*, 60.
- [36] X.-Y. Wang, Z.-H. Jin, B.-W. Gan, S.-W. Lv, M. Xie, W.-H. Huang, *Lab Chip* **2014**, *14*, 2709.
- [37] G. M. Price, K. K. Chu, J. G. Truslow, M. D. Tang-Schomer, A. P. Golden, J. Mertz, J. Tien, *J. Am. Chem. Soc.* **2008**, *130*, 6664.
- [38] Y. Zheng, J. Chen, M. Craven, N. W. Choi, S. Totorica, A. Diaz-Santana, P. Kermani, B. Hempstead, C. Fischbach-Teschl, J. A. López, A. D. Stroock, *Proc. Natl. Acad. Sci. U. S. A.* **2012**, *109*, 9342.
- [39] Y. Ling, J. Rubin, Y. Deng, C. Huang, U. Demirci, J. M. Karp, A. Khademhosseini, *Lab Chip* **2007**, *7*, 756.
- [40] C. J. Bettinger, K. M. Cyr, A. Matsumoto, R. Langer, J. T. Borenstein, D. L. Kaplan, *Adv. Mater.* **2007**, *19*, 2847.
- [41] Y. Qiu, B. Ahn, Y. Sakurai, C. E. Hansen, R. Tran, P. N. Mimche, R. G. Mannino, J. C. Ciciliano, T. J. Lamb, C. H. Joiner, S. F. Ofori-Acquah, W. A. Lam, *Nat. Biomed. Eng.* **2018**, *2*, 453.
- [42] D. T. Chiu, N. L. Jeon, S. Huang, R. S. Kane, C. J. Wargo, I. S. Choi, D. E. Ingber, G. M. Whitesides, *Proc. Natl. Acad. Sci. U. S. A.* **2000**, *97*, 2408.
- [43] A. P. Zhang, X. Qu, P. Soman, K. C. Hribar, J. W. Lee, S. Chen, S. He, *Adv. Mater.* **2012**, *24*, 4266.
- [44] A. M. Kloxin, A. M. Kasko, C. N. Salinas, K. S. Anseth, *Science* **2009**, *324*, 59.
- [45] C. K. Arakawa, B. A. Badeau, Y. Zheng, C. A. DeForest, *Adv. Mater.* **2017**, *29*, 1703156.
- [46] O. Sarig-Nadir, N. Livnat, R. Zajdman, S. Shoham, D. Seliktar, *Biophys. J.* **2009**, *96*, 4743.
- [47] O. Ilina, G.-J. Bakker, A. Vasaturo, R. M. Hofmann, P. Friedl, *Phys. Biol.* **2011**, *8*, 015010.
- [48] C. Arakawa, C. Gunnarsson, C. Howard, M. Bernabeu, K. Phong, E. Yang, C. A. DeForest, J. D. Smith, Y. Zheng, *Sci. Adv.* **2020**, *6*, eaay7243.
- [49] B. Zhang, M. Montgomery, M. D. Chamberlain, S. Ogawa, A. Korolj, A. Pahnke, L. A. Wells, S. Massé, J. Kim, L. Reis, A. Momen, S. S. Nunes, A. R. Wheeler, K. Nanthakumar, G. Keller, M. V. Sefton, M. Radisic, *Nat. Mater.* **2016**, *15*, 669.
- [50] M. P. Cuchiara, A. C. B. Allen, T. M. Chen, J. S. Miller, J. L. West, *Biomaterials* **2010**, *31*, 5491.
- [51] K. C. Hribar, P. Soman, J. Warner, P. Chung, S. Chen, *Lab Chip* **2014**, *14*, 268.
- [52] W. Wu, A. DeConinck, J. A. Lewis, *Adv. Mater.* **2011**, *23*, H178.
- [53] A. Lee, A. R. Hudson, D. J. Shiwardski, J. W. Tashman, T. J. Hinton, S. Yerneni, J. M. Bliley, P. G. Campbell, A. W. Feinberg, *Science* **2019**, *365*, 482.
- [54] D. B. Kolesky, K. A. Homan, M. A. Sklyar-Scott, J. A. Lewis, *Proc. Natl. Acad. Sci. U. S. A.* **2016**, *113*, 3179.
- [55] V. K. Lee, D. Y. Kim, H. Ngo, Y. Lee, L. Seo, S.-S. Yoo, P. A. Vincent, G. Dai, *Biomaterials* **2014**, *35*, 8092.
- [56] V. K. Lee, A. M. Lanzi, H. Ngo, S.-S. Yoo, P. A. Vincent, G. Dai, *Cell. Mol. Bioeng.* **2014**, *7*, 460.
- [57] B. Byambaa, N. Annabi, K. Yue, G. Trujillo-de Santiago, M. M. Alvarez, W. Jia, M. Kazemzadeh-Narbat, S. R. Shin, A. Tamayol, A. Khademhosseini, *Adv. Healthcare Mater.* **2017**, *6*, 1700015.
- [58] T. J. Hinton, Q. Jallerat, R. N. Palchesko, J. H. Park, M. S. Grodzicki, H.-J. Shue, M. H. Ramadan, A. R. Hudson, A. W. Feinberg, *Sci. Adv.* **2015**, *1*, e1500758.
- [59] A. Herland, A. D. van der Meer, E. A. FitzGerald, T.-E. Park, J. J. Sleebloom, D. E. Ingber, *PLoS One* **2016**, *11*, e0150360.
- [60] P. G. Saffman, G. Taylor, *Proc. R. Soc. London, Ser. A* **1958**, *245*, 312.
- [61] J.-H. Huang, J. Kim, N. Agrawal, A. P. Sudarsan, J. E. Maxim, A. Jayaraman, V. M. Ugaz, *Adv. Mater.* **2009**, *21*, 3567.
- [62] G. M. Price, J. Tien, in *Biological Microarrays (Methods in Molecular Biology, Vol. 671)* (Eds: A. Khademhosseini, K.-Y. Suh, M. Zourob), Humana Press, Totowa, NJ **2011**, p. 281.
- [63] B. Trappmann, B. M. Baker, W. J. Polacheck, C. K. Choi, J. A. Burdick, C. S. Chen, *Nat. Commun.* **2017**, *8*, 371.
- [64] H. E. Abaci, Z. Guo, A. Coffman, B. Gillette, W.-H. Lee, S. K. Sia, A. M. Christiano, *Adv. Healthcare Mater.* **2016**, *5*, 1800.
- [65] Y. Seto, R. Inaba, T. Okuyama, F. Sassa, H. Suzuki, J. Fukuda, *Biomaterials* **2010**, *31*, 2209.
- [66] N. Sadr, M. Zhu, T. Osaki, T. Kakegawa, Y. Yang, M. Moretti, J. Fukuda, A. Khademhosseini, *Biomaterials* **2011**, *32*, 7479.
- [67] J. S. Pober, W. Min, J. R. Bradley, *Annu. Rev. Pathol.: Mech. Dis.* **2009**, *4*, 71.
- [68] K. H. K. Wong, J. G. Truslow, A. H. Khankhel, J. Tien, in *Vascularization: Regenerative Medicine and Tissue Engineering* (Ed.: E. M. Brey), CRC Press, Boca Raton, FL **2014**, pp. 109.
- [69] G. M. Price, K. H. K. Wong, J. G. Truslow, A. D. Leung, C. Acharya, J. Tien, *Biomaterials* **2010**, *31*, 6182.
- [70] K. H. K. Wong, J. G. Truslow, J. Tien, *Biomaterials* **2010**, *31*, 4706.
- [71] K. L. S. Chan, A. H. Khankhel, R. L. Thompson, B. J. Coisman, K. H. K. Wong, J. G. Truslow, J. Tien, *J. Biomed. Mater. Res., Part A* **2014**, *102*, 3186.
- [72] R. Gerli, R. Solito, E. Weber, M. Aglianó, *Lymphology* **2000**, *33*, 148.
- [73] S. Y. Yuan, R. R. Rigor, *Regulation of Endothelial Barrier Function*, Morgan & Claypool Life Sciences, San Rafael, CA **2011**.
- [74] R. M. Linville, J. G. DeStefano, M. B. Sklar, Z. Xu, A. M. Farrell, M. I. Bogorad, C. Chu, P. Walczak, L. Cheng, V. Mahairaki, K. A. Wartenby, P. A. Calabresi, P. C. Searson, *Biomaterials* **2019**, *190–191*, 24.
- [75] G. M. Price, K. M. Chrobak, J. Tien, *Microvasc. Res.* **2008**, *76*, 46.
- [76] G. Ligresti, R. J. Nagao, J. Xue, Y. J. Choi, J. Xu, S. Ren, T. Aburatani, S. K. Anderson, J. W. MacDonald, T. K. Bammler, S. M. Schwartz, K. A. Muczynski, J. S. Duffield, J. Himmelfarb, Y. Zheng, *J. Am. Soc. Nephrol.* **2016**, *27*, 2370.
- [77] J. A. Jiménez-Torres, M. Virumbrales-Muñoz, K. E. Sung, M. H. Lee, E. J. Abel, D. J. Beebe, *EBioMedicine* **2019**, *42*, 408.
- [78] S. Alimperti, T. Mirabella, V. Bajaj, W. Polacheck, D. M. Pirone, J. Duffield, J. Eyckmans, R. K. Assoian, C. S. Chen, *Proc. Natl. Acad. Sci. U. S. A.* **2017**, *114*, 8758.
- [79] A. McCurley, S. Alimperti, S. B. Campos-Bilderback, R. M. Sandoval, J. E. Calvino, T. L. Reynolds, C. Quigley, J. W. Mugford, W. J. Polacheck, I. G. Gomez, J. Dovey, G. Marsh, A. Huang, F. Qian, P. H. Weinreb, B. M. Dolinski, S. Moore, J. S. Duffield, C. S. Chen, B. A. Molitoris, S. M. Violette, M. A. Crackower, *J. Am. Soc. Nephrol.* **2017**, *28*, 1741.
- [80] W. J. Polacheck, M. L. Kutys, J. Yang, J. Eyckmans, Y. Wu, H. Vasavada, K. K. Hirschi, C. S. Chen, *Nature* **2017**, *552*, 258.
- [81] P. A. Galie, D.-H. T. Nguyen, C. K. Choi, D. M. Cohen, P. A. Janmey, C. S. Chen, *Proc. Natl. Acad. Sci. U. S. A.* **2014**, *111*, 7968.

- [82] L. L. Bischel, E. W. K. Young, B. R. Mader, D. J. Beebe, *Biomaterials* **2013**, *34*, 1471.
- [83] S. S. Verbridge, A. Chakrabarti, P. Delnero, B. Kwee, J. D. Varner, A. D. Stroock, C. Fischbach, *J. Biomed. Mater. Res., Part A* **2013**, *101*, 2948.
- [84] R. M. Linville, J. G. DeStefano, M. B. Sklar, C. Chu, P. Walczak, P. C. Searson, *J. Cereb. Blood Flow Metab.* **2019**, *40*, 1517.
- [85] E. K. Juang, I. De Cock, C. Keravnou, M. K. Gallagher, S. B. Keller, Y. Zheng, M. Averkiou, *Langmuir* **2019**, *35*, 10128.
- [86] L. L. Bischel, K. E. Sung, J. A. Jiménez-Torres, B. Mader, P. J. Keely, D. J. Beebe, *FASEB J.* **2014**, *28*, 4583.
- [87] L. E. Hind, P. N. Ingram, D. J. Beebe, A. Huttenlocher, *Blood* **2018**, *132*, 1818.
- [88] R. J. Nagao, R. Marcu, Y. Wang, L. Wang, C. Arakawa, C. DeForest, J. Chen, J. A. López, Y. Zheng, *Adv. Sci.* **2019**, *6*, 1901725.
- [89] X. Li, J. Xia, C. T. Nicolescu, M. W. Massidda, T. J. Ryan, J. Tien, *Biofabrication* **2019**, *11*, 014101.
- [90] S. Kotha, S. Sun, A. Adams, B. Hayes, K. T. Phong, R. Nagao, J.-A. Reems, D. Gao, B. Torok-Storb, J. A. López, Y. Zheng, *PLoS One* **2018**, *13*, e0195082.
- [91] S. Massa, M. A. Sakr, J. Seo, P. Bandaru, A. Arneri, S. Bersini, E. Zare-Eelanjegh, E. Jalilian, B.-H. Cha, S. Antona, A. Enrico, Y. Gao, S. Hassan, J. P. Acevedo, M. R. Dokmeci, Y. S. Zhang, A. Khademhosseini, S. R. Shin, *Biomicrofluidics* **2017**, *11*, 044109.
- [92] N. Mori, Y. Morimoto, S. Takeuchi, *Biomaterials* **2017**, *116*, 48.
- [93] B. S. Kim, G. Gao, J. Y. Kim, D.-W. Cho, *Adv. Healthcare Mater.* **2019**, *8*, 1801019.
- [94] N. Y. C. Lin, K. A. Homan, S. S. Robinson, D. B. Kolesky, N. Duarte, A. Moisan, J. A. Lewis, *Proc. Natl. Acad. Sci. U. S. A.* **2019**, *116*, 5399.
- [95] M. A. Roberts, D. Tran, K. L. K. Coulombe, M. Razumova, M. Regnier, C. E. Murry, Y. Zheng, *Tissue Eng., Part A* **2016**, *22*, 633.
- [96] S. G. Rayner, K. T. Phong, J. Xue, D. Lih, S. J. Shankland, E. J. Kelly, J. Himmelfarb, Y. Zheng, *Adv. Healthcare Mater.* **2018**, *7*, 1801120.
- [97] A. D. Wong, P. C. Searson, *Cancer Res.* **2017**, *77*, 6453.
- [98] K. M. Lugo-Cintrón, J. M. Ayuso, B. R. White, P. M. Harari, S. M. Ponik, D. J. Beebe, M. M. Gong, M. Virumbrales-Muñoz, *Lab Chip* **2020**, *20*, 1586.
- [99] M. M. Gong, K. M. Lugo-Cintrón, B. R. White, S. C. Kerr, P. M. Harari, D. J. Beebe, *Biomaterials* **2019**, *214*, 119225.
- [100] V. L. Silvestri, E. Henriët, R. M. Linville, A. D. Wong, P. C. Searson, A. J. Ewald, *Cancer Res.* **2020**, <https://cancerres.aacrjournals.org/content/early/2020/07/14/0008-5472.CAN-19-1564>.
- [101] J. M. Ayuso, R. Truttschel, M. M. Gong, M. Humayun, M. Virumbrales-Munoz, R. Vitek, M. Felder, S. D. Gillies, P. Sondel, K. B. Wisinski, M. Patankar, D. J. Beebe, M. C. Skala, *Oncoimmunology* **2019**, *8*, 1553477.
- [102] C. P. Miller, C. Tsuchida, Y. Zheng, J. Himmelfarb, S. Akilesh, *Neoplasia* **2018**, *20*, 610.
- [103] J. M. Ayuso, M. M. Gong, M. C. Skala, P. M. Harari, D. J. Beebe, *Adv. Healthcare Mater.* **2020**, *9*, 1900925.
- [104] D.-H. T. Nguyen, E. Lee, S. Alimperti, R. J. Norgard, A. Wong, J. J.-K. Lee, J. Eyckmans, B. Z. Stanger, C. S. Chen, *Sci. Adv.* **2019**, *5*, eaav6789.
- [105] T. Mirabella, J. W. MacArthur, D. Cheng, C. K. Ozaki, Y. J. Woo, M. Yang, C. S. Chen, *Nat. Biomed. Eng.* **2017**, *1*, 0083.
- [106] M. A. Redd, N. Zeinstra, W. Qin, W. Wei, A. Martinson, Y. Wang, R. K. Wang, C. E. Murry, Y. Zheng, *Nat. Commun.* **2019**, *10*, 584.
- [107] N. Hibino, G. Villalona, N. Pietris, D. R. Duncan, A. Schoffner, J. D. Roh, T. Yi, L. W. Dobrucki, D. Mejias, R. Sawh-Martinez, J. K. Harrington, A. Sinusas, D. S. Krause, T. Kyriakides, W. M. Saltzman, J. S. Pober, T. Shin'oka, C. K. Breuer, *FASEB J.* **2011**, *25*, 2731.
- [108] M. I. Bogorad, P. C. Searson, *Integr. Biol.* **2016**, *8*, 976.
- [109] E. J. Weber, A. Chapron, B. D. Chapron, J. L. Voellinger, K. A. Lidberg, C. K. Yeung, Z. Wang, Y. Yamaura, D. W. Hailey, T. Neumann, D. D. Shen, K. E. Thummel, K. A. Muczynski, J. Himmelfarb, E. J. Kelly, *Kidney Int.* **2016**, *90*, 627.
- [110] M. Adler, S. Ramm, M. Hafner, J. L. Muhlich, E. M. Gottwald, E. Weber, A. Jaklic, A. K. Ajay, D. Svoboda, S. Auerbach, E. J. Kelly, J. Himmelfarb, V. S. Vaidya, *J. Am. Soc. Nephrol.* **2016**, *27*, 1015.
- [111] K. A. Homan, D. B. Kolesky, M. A. Skylar-Scott, J. Herrmann, H. Obuobi, A. Moisan, J. A. Lewis, *Sci. Rep.* **2016**, *6*, 34845.
- [112] S.-Y. Chang, E. J. Weber, V. S. Sidorenko, A. Chapron, C. K. Yeung, C. Gao, Q. Mao, D. Shen, J. Wang, T. A. Rosenquist, K. G. Dickman, T. Neumann, A. P. Grollman, E. J. Kelly, J. Himmelfarb, D. L. Eaton, *JCI Insight* **2017**, *2*, e95978.
- [113] M. M. Morgan, M. K. Livingston, J. W. Warrick, E. M. Stanek, E. T. Alarid, D. J. Beebe, B. P. Johnson, *Sci. Rep.* **2018**, *8*, 7139.
- [114] L. L. Bischel, D. J. Beebe, K. E. Sung, *BMC Cancer* **2015**, *15*, 12.
- [115] J. M. Ayuso, A. Gillette, K. Lugo-Cintrón, S. Acevedo-Acevedo, I. Gomez, M. Morgan, T. Heaster, K. B. Wisinski, S. P. Palecek, M. C. Skala, D. J. Beebe, *EBioMedicine* **2018**, *37*, 144.
- [116] M. M. Morgan, L. M. Arendt, E. T. Alarid, D. J. Beebe, B. P. Johnson, *FASEB J.* **2019**, *33*, 8623.
- [117] L. J. Barkal, C. L. Procknow, Y. R. Álvarez-García, M. Niu, J. A. Jiménez-Torres, R. A. Brockman-Schneider, J. E. Gern, L. C. Denlinger, A. B. Theberge, N. P. Keller, E. Berthier, D. J. Beebe, *Nat. Commun.* **2017**, *8*, 1770.
- [118] Y. S. Song, R. L. Lin, G. Montesano, N. G. Durmus, G. Lee, S.-S. Yoo, E. Kayaalp, E. Haeggström, A. Khademhosseini, U. Demirci, *Anal. Bioanal. Chem.* **2009**, *395*, 185.
- [119] I. Vollert, M. Seiffert, J. Bachmair, M. Sander, A. Eder, L. Conradi, A. Vogelsang, T. Schulze, J. Uebeler, W. Holthöner, H. Redl, H. Reichenspurner, A. Hansen, T. Eschenhagen, *Tissue Eng., Part A* **2014**, *20*, 854.
- [120] M. Cabodi, V. L. Cross, Z. Qu, K. L. Havenstrite, S. Schwartz, A. D. Stroock, *J. Biomed. Mater. Res., Part B* **2007**, *82B*, 210.
- [121] Y. Zheng, P. W. Henderson, N. W. Choi, L. J. Bonassar, J. A. Spector, A. D. Stroock, *Biomaterials* **2011**, *32*, 5391.
- [122] J. G. Truslow, G. M. Price, J. Tien, *Biomaterials* **2009**, *30*, 4435.
- [123] J. G. Truslow, J. Tien, *Biomicrofluidics* **2011**, *5*, 022201.
- [124] V. Janakiraman, K. Mathur, H. Baskaran, *Ann. Biomed. Eng.* **2007**, *35*, 337.
- [125] M. Durand, *Phys. Rev. E* **2006**, *73*, 016116.



Joe Tien is an associate professor of biomedical engineering at Boston University. He received a B.S. in mathematics and a B.S. in physics, both from the University of California, Irvine, and a Ph.D. in physics from Harvard University. Current research interests include vascularization of biomaterials, quantitative physiology of engineered tissues, biomaterials for microsurgical applications, lymphatics and interstitial transport, inverse problems in vascular imaging, and tumor–vessel interactions.



Yoseph W. Dance is a Ph.D. student in biomedical engineering at Boston University. He received a B.S. in biomedical engineering from Drexel University, with a concentration on biomaterials and tissue engineering. His doctoral research is focused on engineering perfusable, vascularized models of human breast cancer and adipose tissue.